Integrin beta 4 promotes colorectal cancer progression by upregulating Ezrin and activating the Wnt/β-catenin signaling pathway

JING WANG[1*], YI SI[1*], MINGDA XUAN[1*], SHUANGSHUANG HAN[1], KUNYI LIU[1], JIAO JIAO[1], XIAOYAN MEN[1], HONGFEI LI[1], JIA WANG[2], TING LIU[1] and WEIFANG YU[1]

[1]Department of Endoscopy Center, The First Hospital of Hebei Medical University, Shijiazhuang, Hebei 050031, P.R. China; [2]Department of Infectious Diseases, The First Hospital of Hebei Medical University, Shijiazhuang, Hebei 050031, P.R. China

Received December 12, 2025; Accepted May 6, 2026

DOI: 10.3892/ijo.2026.5895

Abstract. Colorectal cancer (CRC) is a major cause of cancer-related mortality worldwide. Integrin beta 4 (ITGB4) has been previously identified as being overexpressed in CRC; however, its precise oncogenic mechanism remains unclear. The present study aimed to elucidate the functional role of ITGB4 in CRC progression and identify its downstream molecular effectors to provide new insights for targeted therapy. The biological functions of ITGB4 were investigated in CRC cell lines (SW480 and HCT116) using a series of *in vitro* assays, including Cell Counting Kit-8, colony formation, Transwell migration and invasion, and flow cytometry for apoptosis following ITGB4 knockdown. An *in vivo* xenograft mouse model was used to evaluate the effect of ITGB4 on tumor growth. Downstream targets were screened using RNA sequencing (RNA-seq) and validated by co-immunoprecipitation and co-immunofluorescence. The underlying signaling pathway was investigated by western blotting and functional rescue experiments. The results demonstrated that knockdown of ITGB4 significantly suppressed CRC cell proliferation, migration and invasion, while promoting apoptosis *in vitro*. Similarly, silencing ITGB4 markedly inhibited tumor growth in the *in vivo* xenograft model. RNA-seq analysis identified Ezrin (EZR) as a key downstream target of ITGB4, and a direct protein-protein interaction was confirmed between them. Mechanistically, ITGB4 knockdown decreased the expression of EZR at both the mRNA and protein levels. ITGB4 was demonstrated to exert its pro-tumorigenic effects through the regulation of EZR, which subsequently activated the Wnt/β-catenin signaling pathway. Interestingly, EZR overexpression partially restored ITGB4 levels, suggesting a hypothetical positive feedback loop via Wnt/β-catenin signaling that could amplify this oncogenic axis. Notably, the malignant phenotypes suppressed by ITGB4 silencing were significantly rescued by the overexpression of EZR. In conclusion, the present study identified a novel ITGB4/EZR/Wnt/β-catenin signaling axis in CRC. ITGB4 promotes CRC progression by modulating EZR expression and subsequently activating the Wnt/β-catenin pathway. These findings highlight ITGB4 as a potential prognostic biomarker and a promising therapeutic target for CRC.

Correspondence to: Professor Weifang Yu or Dr Ting Liu, Department of Endoscopy Center, The First Hospital of Hebei Medical University, 89 Donggang Road, Shijiazhuang, Hebei 050031, P.R. China
E-mail: yuweifang@hebmu.edu.cn
E-mail: 59103696@hebmu.edu.cn

*Contributed equally

Abbreviations: CRC, colorectal cancer; ITGB4, integrin beta 4; EZR, ezrin; CCK-8, Cell Counting Kit-8; RNA-seq, RNA sequencing; Co-IP, co-immunoprecipitation; Co-IF, co-immunofluorescence; DMEM, Dulbecco's Modified Eagle's Medium; FBS, fetal bovine serum; siRNA, small interfering RNA; shRNA, short hairpin RNA; RT-qPCR, reverse transcription-quantitative polymerase chain reaction; IHC, immunohistochemistry; DEGs, differentially expressed genes; TCGA, The Cancer Genome Atlas

Key words: CRC, ITGB4, EZR, Wnt/β-catenin signaling, metastasis, prognostic biomarker, therapeutic target

Introduction

Metastasis remains the primary cause of mortality in patients with colorectal cancer (CRC) (1). The metastatic cascade is a complex, multi-step process initiated by the detachment of cancer cells from the primary tumor, a step heavily regulated by cell-matrix adhesion molecules (2). Alterations in the expression of integrins and their interactions with the extracellular matrix (ECM) are fundamental to this process, allowing tumor cells to acquire invasive properties (3). Consequently, there is an urgent need to identify novel therapeutic targets that can inhibit the proliferation, invasion and migration of CRC cells. The advent of high-throughput technologies and public biological databases has accelerated research into the genetic and epigenetic alterations driving CRC, revealing that specific gene mutations are pivotal to its pathogenesis (4). In-depth investigation of these aberrantly expressed genes is crucial for

understanding CRC biology and developing effective strategies for early diagnosis and precision treatment.

The authors' research group previously identified Integrin Beta 4 (ITGB4) as a gene of significant diagnostic and therapeutic potential in CRC, leveraging advanced technologies such as mass cytometry (CyTOF), gene chips and protein arrays. This discovery led to a national invention patent (Patent Number: ZL 2017 1 1148747.1) (5). ITGB4, a member of the integrin family, is predominantly expressed on the basal surface of epithelial cells and forms hemidesmosomes by dimerizing with integrin alpha 6 (ITGA6) (6). Accumulating evidence indicates that ITGB4 is overexpressed in various malignancies, including breast, bladder, cervical, head and neck, lung and pancreatic cancers, where its expression often correlates with tumor invasion and poor prognosis (7-14). The authors' prior studies corroborated these findings in CRC, demonstrating that elevated ITGB4 levels in both tissues and serum are associated with adverse clinicopathological features and reduced overall survival (OS) (15,16). Gene co-expression analysis suggested that ITGB4's regulatory role in CRC involves multiple signaling pathways related to cell proliferation, migration and apoptosis. However, the specific molecular mechanism through which ITGB4 functions in CRC has not been fully elucidated.

Integrins act as critical biomechanical sensors that relay signals by connecting the ECM to the intracellular actin cytoskeleton (17). This linkage is often mediated by scaffolding proteins such as the Ezrin-Radixin-Moesin (ERM) family, which crosslink actin filaments to plasma membrane proteins to regulate cell polarity, adhesion and migration (18). Given this functional synergy, it was hypothesized that ITGB4 might orchestrate CRC progression through specific interactions with cytoskeletal linkers such as Ezrin (EZR). The present study aimed to systematically investigate the role of ITGB4 in the initiation and progression of CRC. Its oncogenic functions were first validated *in vitro* and *in vivo*. Subsequently, through RNA sequencing (RNA-seq) and a multi-step bioinformatic filtering process, EZR was identified as a novel downstream target of ITGB4. It was demonstrated that ITGB4 interacts with and positively regulates the expression of EZR, thereby activating the Wnt/β-catenin signaling pathway to promote CRC progression. The findings of the present study delineate the ITGB4/EZR/Wnt/β-catenin axis as a critical regulatory network in CRC, offering a potential new target for precision therapeutic intervention.

Materials and methods

Cell culture. The human CRC cell lines SW480 (cat. no. CCL-228™) and HCT116 (cat. no. CCL-247™) were purchased from the American Type Culture Collection. Cells were cultured in Dulbecco's Modified Eagle's Medium (DMEM; Gibco; Thermo Fisher Scientific, Inc.) supplemented with 10% fetal bovine serum (FBS; Gibco; Thermo Fisher Scientific, Inc.) and 1% penicillin-streptomycin. Cultures were maintained in a humidified incubator at 37˚C with 5% CO_2. All cells used in experiments were in the logarithmic growth phase. Cell line authentication was performed prior to the study, and routine testing confirmed the absence of mycoplasma contamination.

Small interfering (siRNA), short hairpin (shRNA), plasmids and transfections. For transient knockdown, siRNAs targeting ITGB4 (siITGB4) and a negative control siRNA (siNC) were synthesized by Shanghai GenePharma Co., Ltd. For EZR overexpression, a human EZR open reading frame was cloned into the pcDNA3.1 vector (pcDNA3.1-EZR), with the empty vector serving as a control (pcDNA3.1-vector); these were also obtained from Shanghai GenePharma Co., Ltd. For stable knockdown, shRNAs targeting ITGB4 (shITGB4) and a non-targeting control (shNC) were cloned into a lentiviral vector by Shanghai GenePharma Co., Ltd. The sequences for all siRNAs and shRNAs used are listed in Table SI. Transfections were performed using Lipofectamine 3000 (Invitrogen; Thermo Fisher Scientific, Inc.) according to the manufacturer's protocol when cell confluence reached 80-90%. For experiments performed in 6-well plates, 1.2 μg of plasmid or 50 nM of siRNA was transfected per well. The transfection was performed at 37˚C for 6-8 h. Following transfection, subsequent experiments were performed after 24 h (for RNA extraction) or 48 h (for protein extraction).

Generation of stable cell lines. To establish stable ITGB4-knockdown cell lines, HCT116 cells, cultured to 70% confluence, were transfected with shITGB4 or shNC vectors. A total of 48 h post-transfection, the cells were subjected to selection with 600 μg/ml G418 (Neomycin). The selection medium was refreshed every 2-3 days. After ~1 week, when significant cell death was observed, the G418 concentration was reduced to 300 μg/ml for maintenance. After 10-14 days of selection, resistant cell colonies were pooled, expanded, and cultured without G418. The efficiency of stable knockdown was confirmed by reverse transcription-quantitative PCR (RT-qPCR) and western blot analysis.

RNA extraction and RT-qPCR. Total RNA was extracted from cells using the RNA-Easy Kit (Vazyme Biotech Co., Ltd.). cDNA was synthesized from 1 μg of total RNA using the PrimeScript RT Reagent Kit (Takara Biotechnology Co., Ltd.) according to the manufacturer's instructions. RT-qPCR was performed on a 4800 Real-Time PCR System using SYBR Green Master Mix (Vazyme Biotech Co., Ltd.). The thermal cycling conditions were: 95˚C for 5 min, followed by 40 cycles of 95˚C for 10 sec and 60˚C for 30 sec. Relative gene expression was calculated using the $2^{-\Delta\Delta Cq}$ method (19), with β-actin serving as the internal control. Primer sequences are listed in Table SII.

Western blot analysis. Cells were lysed in RIPA buffer (Beijing Solarbio Science & Technology Co., Ltd.) supplemented with a protease inhibitor cocktail (PMSF; Beijing Solarbio Science & Technology Co., Ltd.). Protein concentrations were determined using a BCA protein assay kit (Beijing Solarbio Science & Technology Co., Ltd.). Equal amounts of protein (30 μg) were separated by 10% SDS-PAGE and transferred to polyvinylidene fluoride membranes (Merck KGaA). The membranes were blocked with 5% non-fat milk in TBST (0.1% Tween-20) for 1 h at room temperature and then incubated overnight at 4˚C with primary antibodies. The primary antibodies used were: anti-ITGB4 (1:1,000; cat. no. ab261778; Abcam), anti-EZR (1:1,000; cat. no. 26056-1-AP; Proteintech Group,

Inc.), anti-β-catenin (1:1,000; cat. no. 51067-2-AP; Proteintech Group, Inc.), anti-c-Myc (1:1,000; cat. no. 10828-1-AP; Proteintech Group, Inc.), anti-cyclin D1 (1:500; cat. no. 60186-1-Ig; Proteintech Group, Inc.) and anti-β-actin (1:1,500; cat. no. TA-09; ZSBG-Bio; http://www.zsbio.com). After washing, membranes were incubated with corresponding HRP-conjugated secondary antibodies (1:2,500; cat. no. A23920; Abbkine Scientific Co., Ltd.). Immunoreactive bands were visualized using an Odyssey scanning system (LI-COR Biosciences). Band intensities were quantified using ImageJ software (version 1.53k; National Institutes of Health).

Cell proliferation assays. For the Cell Counting Kit-8 (CCK-8) assay, cells were seeded into 96-well plates at a density of $1x10^3$ cells/well. At 24, 48, 72 and 96 h, 10 μl of CCK-8 reagent (Dojindo Laboratories, Inc.) was added to each well, followed by a 2 h incubation at 37˚C. The absorbance at 450 nm was measured using a microplate reader (Promega Corporation). For the colony formation assay, cells were seeded into 6-well plates at 500 cells/well and cultured for 10-14 days, with the medium changed every 3 days. Colonies were fixed with 4% paraformaldehyde (PFA) at room temperature for 30 min, stained with 0.1% crystal violet at room temperature for 15 min, and colonies containing >50 cells were counted.

Cell migration and invasion assays. For the wound healing assay, cells were cultured to 100% confluence in 6-well plates. A scratch was made using a 200-μl pipette tip. After washing with PBS, cells were cultured in serum-free medium. Images were captured at 0 and 48 h. The migration rate was calculated based on the change in wound width. For Transwell assays, $1x10^5$ cells in 200 μl of serum-free medium were seeded into the upper chamber of a Transwell insert (8.0 μm pore size; Corning, Inc.). The lower chamber contained 700 μl of DMEM with 10% FBS. For the invasion assay, the upper chamber was pre-coated with Matrigel (BD Biosciences) at 37˚C for 2 h. After 48 h of incubation, non-migratory/invasive cells were removed from the upper surface. Cells on the lower surface were fixed with 4% PFA at room temperature for 30 min, stained with 0.1% crystal violet at room temperature for 20 min, and counted in five random fields under a light microscope.

Apoptosis assay. Cell apoptosis was assessed using the Annexin V-FITC/PI Apoptosis Detection Kit (Neobioscience Technology Co., Ltd.). After 48 h of transfection, cells were harvested, washed with PBS, and resuspended in binding buffer. Cells were then stained with Annexin V-FITC and Propidium Iodide (PI) for 15 min in the dark. The percentage of apoptotic cells was determined by flow cytometry (BD Biosciences) and analyzed using FlowJo software (version 10; BD Biosciences).

Animal studies. A total of 12 5-week-old male BALB/c nude mice, weighing 18-22 g, were housed in a specific pathogen-free (SPF) facility under a 12/12-h light/dark cycle with free access to food and water. They were randomly divided into two groups (n=6 per group). HCT116 cells ($2x10^6$) stably expressing shNC or shITGB4 were suspended in 100 μl of serum-free DMEM and injected subcutaneously into the right flank of each mouse. Tumor growth was monitored every 3 days by measuring the length (L) and width (W) with calipers. Tumor volume was calculated using the formula: $V=(L \times W^2)/2$. After 21 days, all animals were euthanized by cervical dislocation after anesthesia with intraperitoneal injection of 40-50 mg/kg sodium pentobarbital, and tumors were excised, weighed, and processed for histological analysis. Tumors were fixed at 4˚C overnight in 4% PFA for subsequent H&E and immunohistochemistry (IHC) staining. The study protocols were approved by the Experimental Animal Care and Use Committee and Ethics Committee of The First Hospital of Hebei Medical University (approval no. 20220395; Shijiazhuang, China).

RNA sequencing (RNA-seq) and bioinformatic analysis. Total RNA was extracted from SW480 cells transfected with siNC or siITGB4 (three biological replicates per group) using TRIzol™ reagent (cat. no. 5596026CN; Thermo Fisher Scientific, Inc.). RNA quality and integrity were verified using the Agilent 2100 Bioanalyzer. The type of sequencing was paired-end, with a nucleotide length of 150 bp, with TruSeq RNA Exome Kit (cat. no. RS-301-2001; Illumina, Inc.) used for sequencing. Library construction and sequencing were performed by Novogene Technology Co., Ltd. on an Illumina NovaSeq 6000 platform. The loading concentration of the final library was 1.5 ng/μl and was measured using a Qubit 2.0 Fluorometer. After quality control, clean reads were aligned to the human reference genome (GRCh38). Differential expression analysis was performed using DESeq2 (version 1.20.0). Genes with an adjusted $P<0.05$ and a $|\log2\text{Fold Change}| >1.0$ were considered differentially expressed genes (DEGs).

IHC. Paraffin-embedded tumor sections (4 μm) were deparaffinized with xylene, rehydrated using ethanol series, and subjected to antigen retrieval. Sections were then incubated with an anti-Ki67 antibody (1:100; cat. no. 27309-1-AP; Proteintech Group, Inc.) overnight at 4˚C. Staining was performed using a two-step detection kit (ZSBG-Bio) and visualized with DAB. Images were captured using a light microscope, and the staining intensity was quantified as the average optical density using ImageJ software.

Co-immunoprecipitation (Co-IP) and Co-immunofluorescence (Co-IF). For Co-IP, SW480 cell lysates were incubated with anti-ITGB4 antibody (10 μg; Proteintech Group, Inc.), anti-EZR antibody (10 μg; Proteintech Group, Inc.), or control IgG (10 μg; Proteintech Group, Inc.) using the Pierce™ Classic Magnetic IP/Co-IP Kit (cat. no. 88804; Thermo Fisher Scientific, Inc.) according to the manufacturer's instructions. Immunoprecipitated proteins were analyzed by western blotting. For Co-IF, SW480 cells cultured on glass coverslips were fixed with 4% PFA at room temperature for 30 min, permeabilized with 0.2% Triton X-100, and blocked with 2% BSA at room temperature for 30 min. Cells were then incubated with primary antibodies against ITGB4 (1:50; cat. no. sc-13543; Santa Cruz Biotechnology, Inc.) and EZR (1:50; cat. no. 26056-1-AP; Proteintech Group, Inc.) overnight at 4˚C. After washing, cells were incubated with Cy3-conjugated anti-rabbit and FITC-conjugated anti-mouse secondary antibodies (cat. nos. A0516 and A0568; Beyotime Institute of Biotechnology. Nuclei were counterstained

with DAPI (1 mg/ml; cat. no. C1002; Beyotime Institute of Biotechnology). Images were acquired using a Zeiss laser scanning confocal microscope (Carl Zeiss AG).

Public database analysis. ITGB4 expression data in CRC and adjacent normal tissues were obtained from The Cancer Genome Atlas (TCGA) and Gene Expression Profiling Interactive Analysis 2 (GEPIA2; http://gepia2.cancer-pku.cn/) databases. The TCGA and GEPIA2 datasets were prioritized due to their large sample sizes, standardized high-throughput sequencing platforms, and comprehensive clinical annotations, which provide robust statistical power for differential expression and survival analyses compared with smaller, individual datasets. Inclusion criteria involved datasets containing paired tumor and adjacent normal tissues with complete follow-up information. Although clinicopathological variables such as tumor stage and subtype are available in these datasets, the current analysis focused on overall differential expression and survival correlations to identify potential targets, without stratification by specific parameters. The prognostic value of gene expression was assessed using the Kaplan-Meier plotter (https://kmplot.com/analysis/) followed by the log-rank test. Subcellular localization data were retrieved from GeneCards (https://www.genecards.org/). STRING database (https://string-db.org/) was used for PPI interaction network.

Statistical analysis. All experiments were performed with at least three independent replicates. Data are presented as the mean ± standard deviation (SD). Statistical analyses were performed using GraphPad Prism 8.0 (Dotmatics) and SPSS 21.0 (IBM Corp.). Differences between two groups were analyzed using an unpaired two-tailed Student's t-test. Comparisons among multiple groups were performed using one-way or two-way ANOVA followed by Bonferroni post-hoc test. $P<0.05$ was considered to indicate a statistically significant difference.

Results

ITGB4 is upregulated in CRC and correlates with poor prognosis. To corroborate previous findings, ITGB4 expression was first analyzed using public databases. Analysis of TCGA and GEPIA2 datasets confirmed that ITGB4 mRNA expression was significantly higher in CRC tissues compared with adjacent normal tissues (Fig. 1A-C). Furthermore, Kaplan-Meier survival analysis revealed that patients with high ITGB4 expression had significantly poorer OS than those with low expression (Fig. 1D). These results are consistent with the authors' prior study (6) and collectively underscore that ITGB4 is an oncogenic factor in CRC, and its overexpression is associated with unfavorable patient outcomes, highlighting its potential as a prognostic biomarker.

Downregulation of ITGB4 suppresses malignant phenotypes of CRC cells in vitro. To investigate the biological function of ITGB4 in CRC, its expression in SW480 and HCT116 cells was first silenced using siRNAs. Four different siRNA sequences were tested, and the siITGB4-681 sequence, which demonstrated the most potent knockdown efficiency at both mRNA and protein levels, was selected for subsequent experiments (Fig. 2A and B). Transient transfection with siITGB4-681 effectively reduced ITGB4 mRNA and protein expression in both cell lines (Fig. 2C-F). Functional assays revealed that ITGB4 knockdown significantly inhibited cell proliferation, as determined by CCK-8 assays (Fig. 2G and H), and suppressed clonogenic ability, as shown by colony formation assays (Fig. 2I and J). Moreover, flow cytometric analysis indicated that ITGB4 silencing significantly increased the proportion of apoptotic cells (Fig. 2K and L). Transwell assays demonstrated a significant reduction in both the migratory and invasive capacities of CRC cells upon ITGB4 knockdown (Fig. 2M and N). Collectively, these *in vitro* results suggest that ITGB4 plays a critical role in promoting CRC cell proliferation, survival, migration and invasion.

Knockdown of ITGB4 inhibits CRC growth in vivo. To extend the *in vitro* findings, the role of ITGB4 in tumor growth was assessed using a xenograft model. An HCT116 cell line with stable ITGB4 knockdown (shITGB4) was established, confirming sustained suppression of ITGB4 expression (Fig. 3A and B). These cells, along with control cells (shNC), were subcutaneously injected into nude mice. Tumor growth was monitored over 21 days. The tumors formed by shITGB4 cells grew significantly slower and were substantially smaller and lighter at the end of the experiment compared with tumors from the shNC group (Fig. 3C-F). The reduced ITGB4 expression in the xenograft tumors was verified by RT-qPCR and western blotting (Fig. 3G and H). H&E staining confirmed the CRC tissue morphology in the tumors (Fig. 3I). Furthermore, IHC staining for the proliferation marker Ki-67 showed significantly lower positivity in the shITGB4 group, indicating reduced cell proliferation (Fig. 3J and K). These *in vivo* data provide strong evidence that ITGB4 is essential for promoting CRC tumorigenesis.

Identification of EZR as a downstream target of ITGB4 in CRC. To uncover the molecular mechanisms downstream of ITGB4, RNA-seq was performed on SW480 cells following ITGB4 knockdown. This analysis identified 572 DEGs, of which 296 were downregulated and 276 were upregulated (Fig. 4A and B). To pinpoint key downstream effectors, a stringent, multi-step filtering strategy was devised. First, focus was addressed on the 296 downregulated genes from our RNA-seq data. This list was then intersected with two externally derived gene sets: (i) Genes known to be co-expressed with ITGB4 in CRC patient cohorts (from the GEPIA database) and (ii) genes that are significantly upregulated in CRC tissues compared with normal tissues (from the GEPIA2 database). This intersection yielded a refined list of 35 candidate genes. To further narrow the selection, genes whose protein products share a subcellular localization with ITGB4 (that is, plasma membrane or cytoplasm, based on GeneCards data), were prioritized. This criterion was selected because ITGB4 is a transmembrane receptor; therefore, its immediate downstream signal transducers are likely to be physically proximal, residing at the membrane or in the sub-membrane cortical cytoplasm. This systematic process identified five high-confidence candidate target genes: ITGA6, CXADR, EZR, GPRC5C and EPHA2 (Fig. 4C). The regulatory relationship was validated by confirming that knockdown of ITGB4 led to a significant

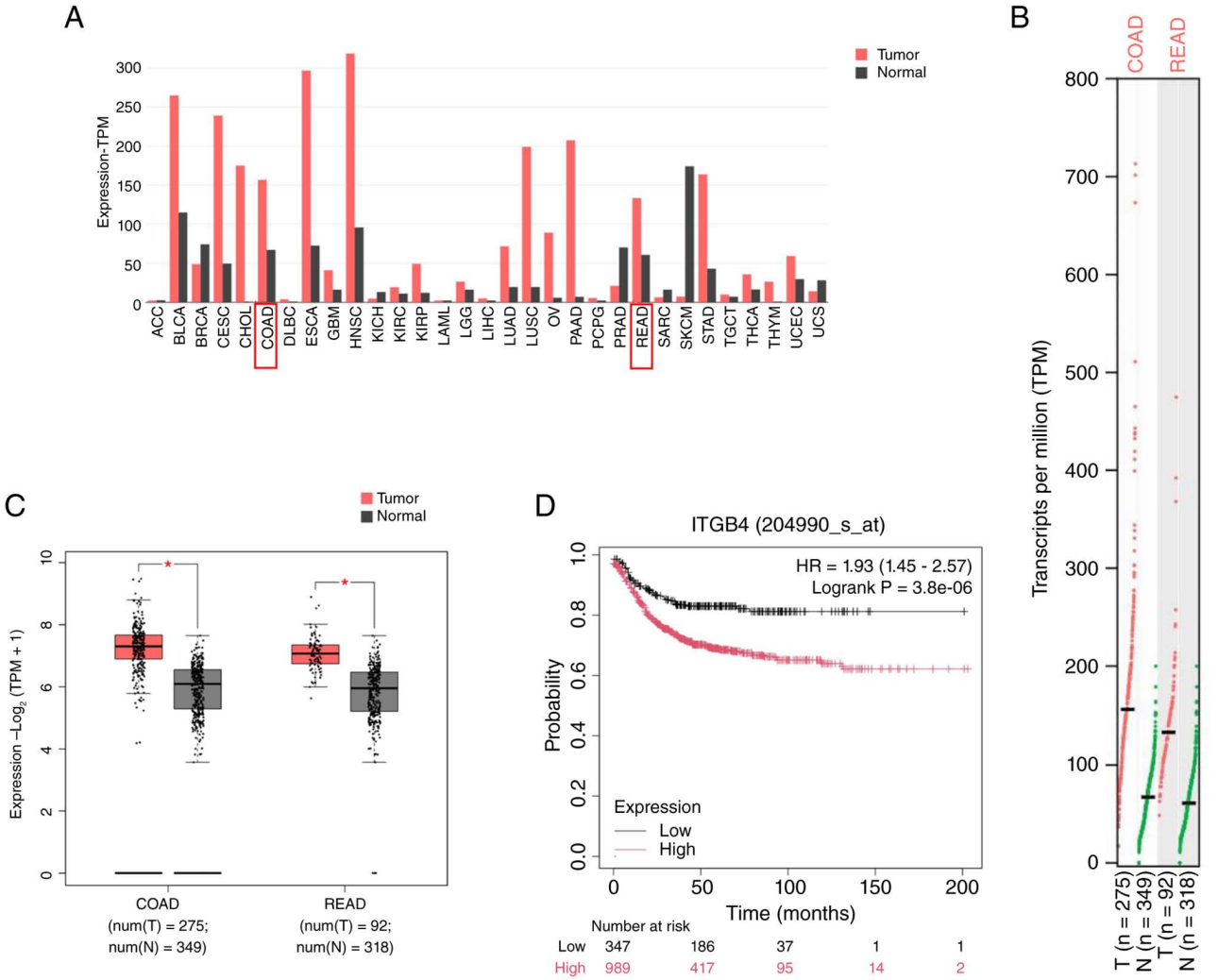

Figure 1. ITGB4 is upregulated in CRC and associated with poor prognosis. (A-C) Analysis of ITGB4 mRNA expression in CRC tissues and adjacent normal tissues using The Cancer Genome Atlas and GEPIA2 databases. (D) Kaplan-Meier analysis demonstrating the correlation between ITGB4 expression levels and overall survival in patients with CRC. *P<0.05. ITGB4, integrin beta 4; CRC, colorectal cancer; COAD, colon adenocarcinoma; READ, rectum adenocarcinoma; HR, hazard ratio.

decrease in the mRNA levels of all five candidate genes in both SW480 and HCT116 cells (Fig. 4D and E). Among the candidates, EZR, CXADR and ITGA6 showed predominantly plasma membrane localization, similar to ITGB4, whereas GPRC5C showed mixed localization. This spatial proximity is a prerequisite for direct protein-protein interaction (PPI). Among these candidates, EZR was selected for further investigation based on its strong positive correlation with ITGB4 expression in CRC patient samples (Fig. 5C), its consistent upregulation in CRC tissues (Fig. 5B), its shared subcellular localization (Fig. 5A) and its strong association with poor patient prognosis (Fig. 5D), which mirrored the prognostic significance of ITGB4.

ITGB4 interacts with and positively regulates the expression of EZR. Given the strong correlational evidence, a potential physical interaction between ITGB4 and EZR was next investigated. Co-IP assays in SW480 cells demonstrated that endogenous ITGB4 could be immunoprecipitated with an anti-EZR antibody, and conversely, EZR was pulled down with an anti-ITGB4 antibody, confirming that the two proteins exist in the same complex (Fig. 6A). Co-IF staining further revealed that ITGB4 and EZR extensively co-localize at the plasma membrane of CRC cells (Fig. 6B). This interaction is also supported by PPI network analysis from the STRING database (Fig. 6C). It was then confirmed that ITGB4 regulates EZR expression. As shown in Fig. 6F and G, knockdown of ITGB4 in SW480 cells resulted in a significant reduction of both EZR mRNA and protein levels. To assess the functional hierarchy, rescue experiments were performed. After establishing an efficient EZR overexpression system (Fig. 6D and E), cells were co-transfected with siITGB4 and the EZR overexpression plasmid. Interestingly, overexpression of EZR partially restored the suppressed levels of ITGB4 mRNA and protein induced by siITGB4 (Fig. 6H and I). Given that EZR functions as a downstream effector that activates Wnt/β-catenin signaling, this concomitant increase in ITGB4 suggests the potential existence of a positive feedback loop. It was hypothesized that hyperactive Wnt/β-catenin signaling may transcriptionally upregulate ITGB4 to further sustain the malignant progression. Collectively, these data establish that ITGB4 interacts with EZR and positively regulates its expression at both transcriptional and post-transcriptional levels.

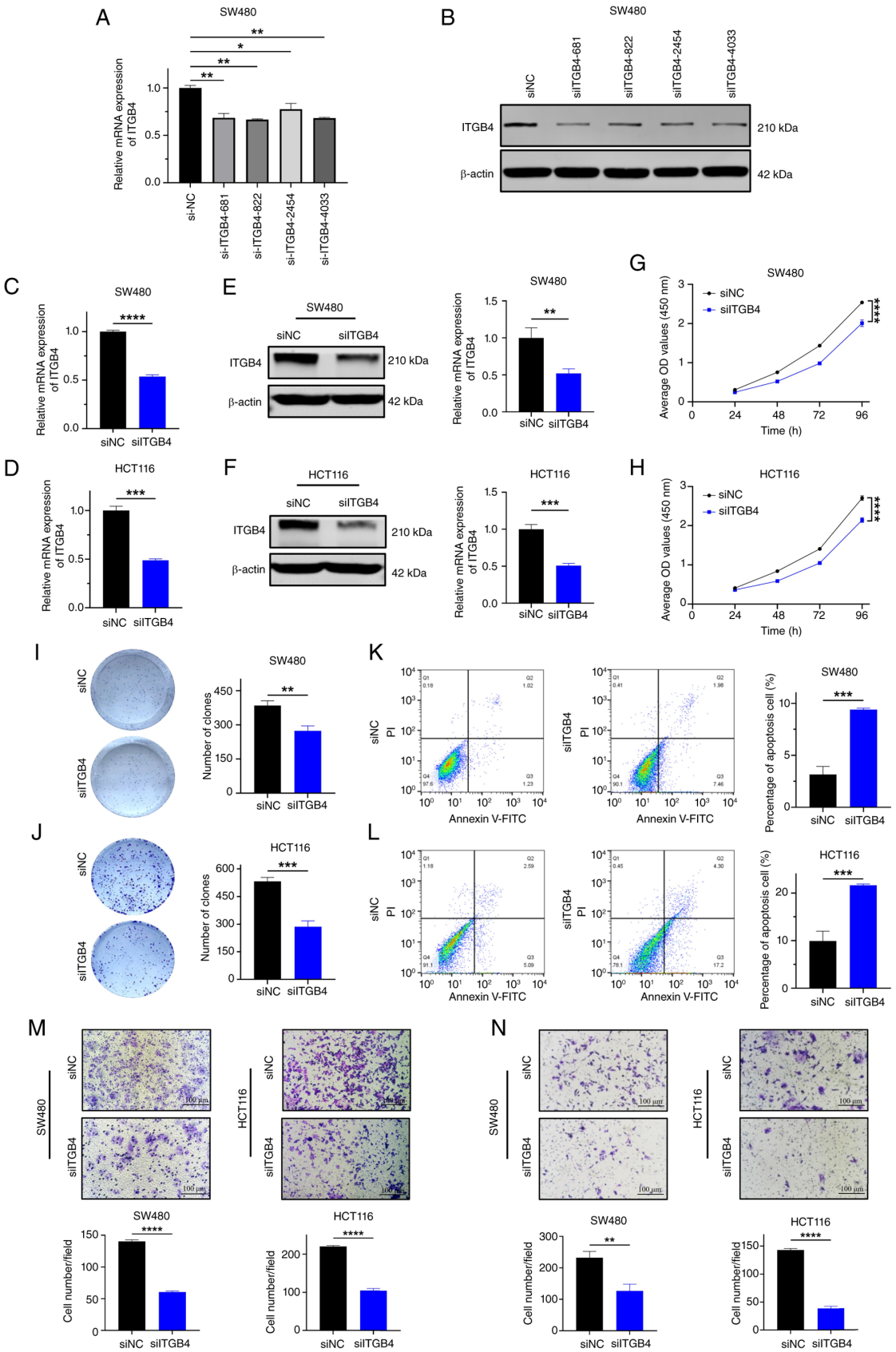

Figure 2. Knockdown of ITGB4 inhibits proliferation, migration and invasion and promotes apoptosis in CRC cells. (A) RT-qPCR validation of knockdown efficiency for four different siITGB4 sequences in SW480 cells. (B) Western blot validation of knockdown efficiency for the four siITGB4 sequences. (C and D) Verification of siITGB4 knockdown efficiency at the mRNA level in SW480 and HCT116 cells via RT-qPCR. (E and F) Verification of siITGB4 knockdown efficiency at the protein level via western blotting. (G and H) Cell Counting Kit-8 assays showing the effect of ITGB4 knockdown on the proliferation of SW480 and HCT116 cells. (I and J) Colony formation assays demonstrating the effect of ITGB4 knockdown on the clonogenic ability of CRC cells. (K and L) Flow cytometric analysis showing the effect of ITGB4 knockdown on apoptosis. (M and N) Transwell assays showing the effect of ITGB4 knockdown on the migration and invasion abilities of SW480 and HCT116 cells (Scale bar, 100 μm). Data are presented as the mean ± SD. *P<0.05, **P<0.01, ***P<0.001 and ****P<0.0001. ITGB4, integrin beta 4; CRC, colorectal cancer; RT-qPCR, reverse transcription-quantitative PCR; si-, small interfering; NC, negative control.

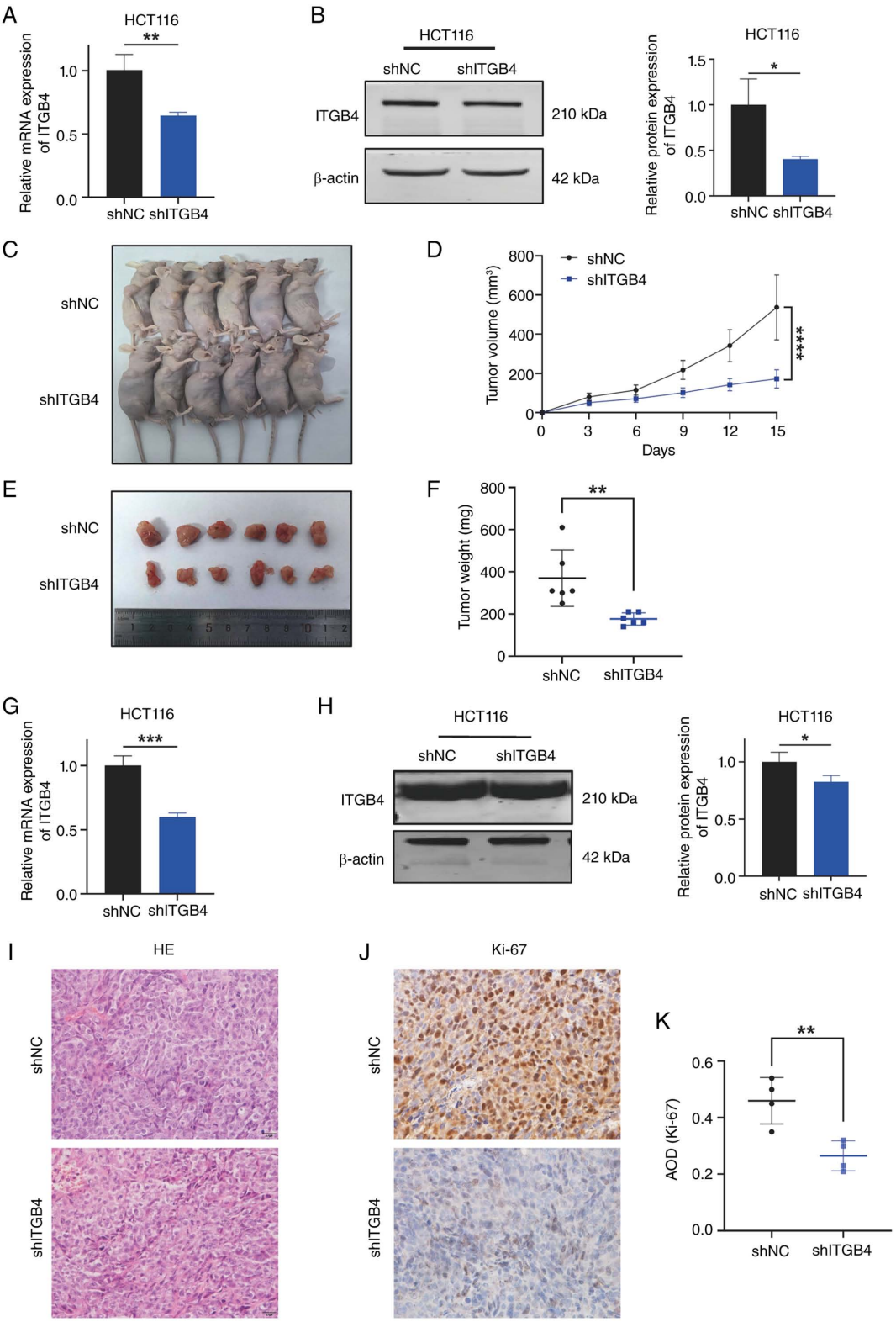

Figure 3. ITGB4 silencing suppresses colorectal cancer growth *in vivo*. (A and B) Reverse transcription-quantitative PCR and western blot analysis verifying the stable knockdown efficiency of shITGB4 in HCT116 cells. (C) Representative images of tumor-bearing nude mice from the shNC and shITGB4 groups. (D) Tumor growth curves for both groups over 21 days. (E and F) Images and weights of the excised xenograft tumors. (G and H) Verification of ITGB4 knockdown in xenograft tumor tissues. (I) Representative H&E staining of tumor sections (scale bars, 50 μm). (J and K) Representative immunohistochemical staining and quantification of Ki-67 in tumor sections (scale bars, 50 μm). Data are presented as the mean ± SD. *P<0.05, **P<0.01, ***P<0.001 and ****P<0.0001. ITGB4, integrin beta 4; sh-, short hairpin; NC, negative control; AOD, average optical density.

ITGB4 promotes CRC progression by regulating EZR to activate the Wnt/β-catenin signaling pathway. To determine the signaling pathway through which the ITGB4/EZR axis functions, Kyoto Encyclopedia of Genes and Genomes pathway enrichment analysis was performed on the DEGs from the current RNA-seq data. The analysis revealed a

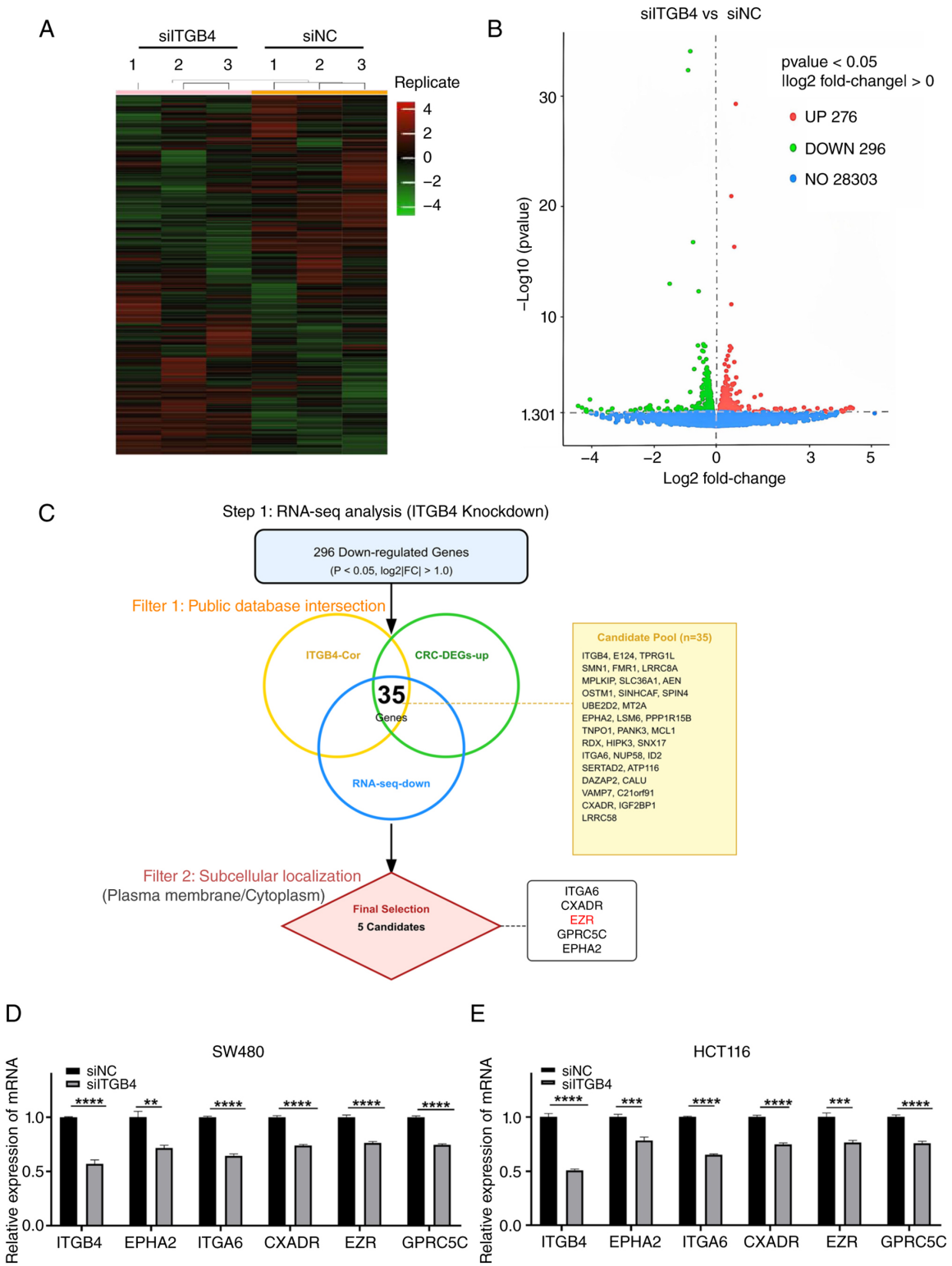

Figure 4. Systematic screening identifies candidate downstream targets of ITGB4. (A) Heatmap of DEGs identified by RNA-seq analysis of SW480 cells after ITGB4 knockdown. (B) Volcano plot illustrating the distribution of DEGs. (C) Schematic flowchart illustrating the multi-step filtering strategy. A Venn diagram was used to intersect ITGB4-downregulated genes (from RNA-seq) with genes co-expressed with ITGB4 and upregulated in colorectal cancer (from public databases), identifying 35 candidate genes. These candidates were further filtered by subcellular localization to identify the final five targets. (D and E) Reverse transcription-quantitative PCR validation of the mRNA levels of the five candidate target genes following ITGB4 knockdown in SW480 and HCT116 cells. **P<0.01, ***P<0.001 and ****P<0.0001. ITGB4, integrin beta 4; DEGs, differentially expressed genes; RNA-seq, RNA sequencing; si-, small interfering; NC, negative control; EZR, Ezrin.

significant enrichment in the Wnt/β-catenin signaling pathway (Fig. 7A). To validate this, key proteins of the pathway were examined by western blotting. ITGB4 knockdown in HCT116 cells led to a marked decrease in the levels of active β-catenin and its downstream transcriptional targets, c-Myc and Cyclin D1. Crucially, this downregulation was reversed by the ectopic

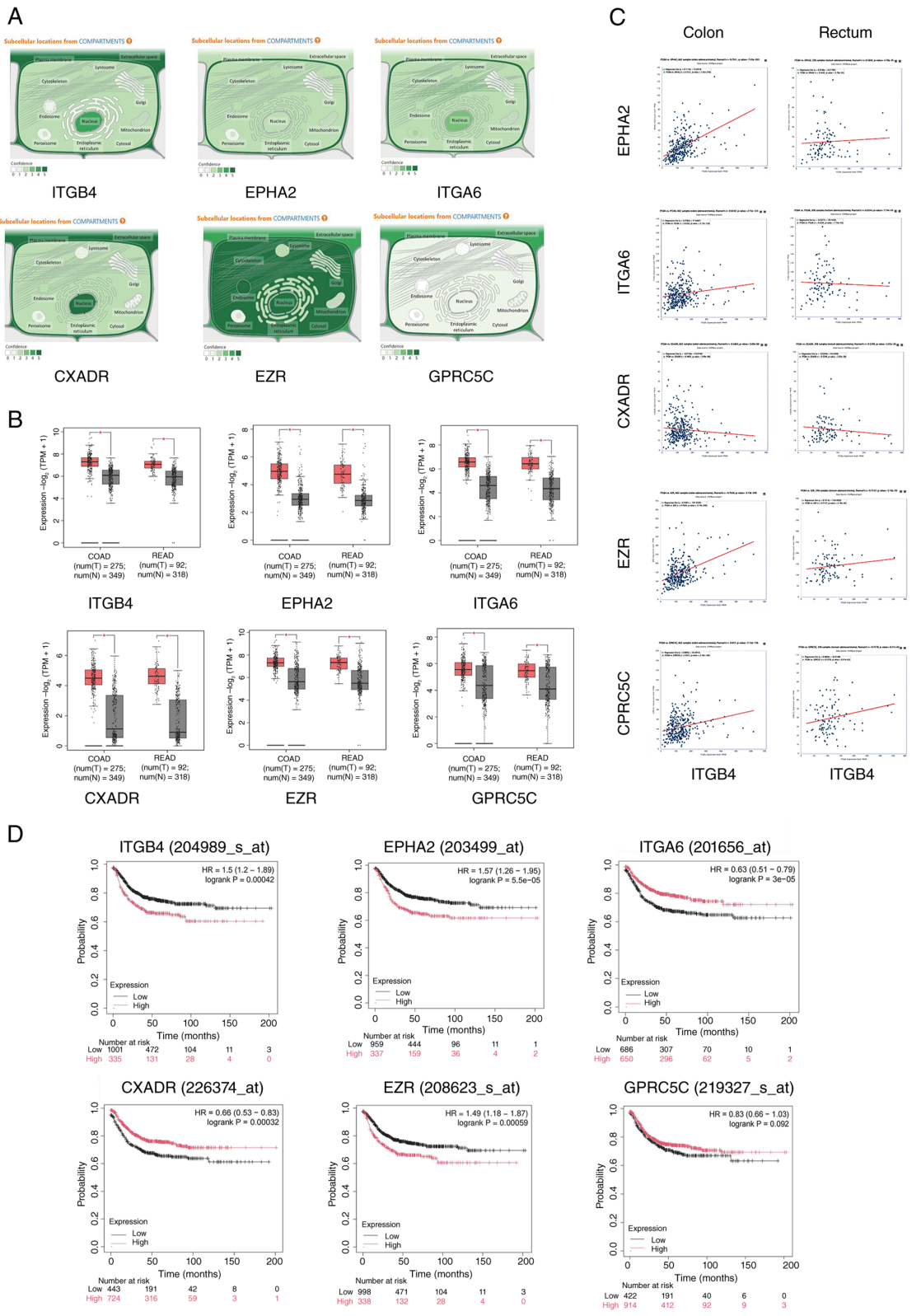

Figure 5. Bioinformatic analysis highlights EZR as a prime candidate downstream of ITGB4. (A) Subcellular localization of ITGB4 and the five candidate genes as annotated in the GeneCards database. (B) Expression analysis of the five candidate genes in CRC vs. adjacent normal tissues using the GEPIA2 database. (C) Correlation analysis of ITGB4 expression with each of the five candidate genes in The Cancer Genome Atlas-Colon Adenocarcinoma cohort. (D) Kaplan-Meier survival analysis showing the prognostic significance of the five candidate genes in patients with CRC. *P<0.05. EZR, Ezrin; ITGB4, integrin beta 4; CRC, colorectal cancer; HR, hazard ratio.

overexpression of EZR (Fig. 7B). This indicates that ITGB4 activates the Wnt/β-catenin pathway in an EZR-dependent manner. Finally, functional rescue experiments were conducted to confirm that EZR mediates the oncogenic effects of ITGB4. As revealed in Fig. 7C-K, while ITGB4 knockdown suppressed CRC cell proliferation, migration and invasion, concomitant

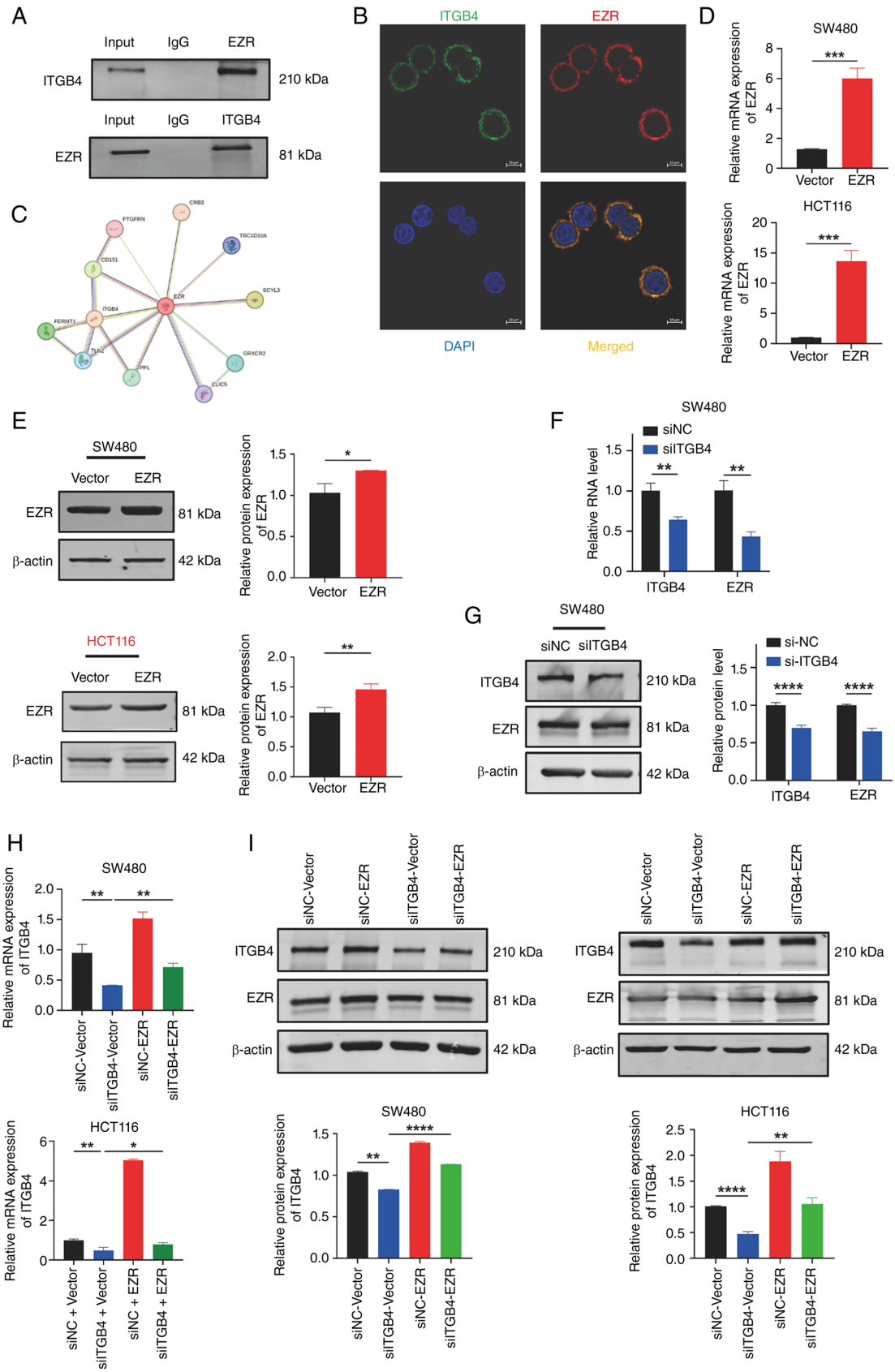

Figure 6. ITGB4 interacts with EZR and regulates its expression. (A) Co-immunoprecipitation assay in SW480 cells demonstrating the interaction between endogenous ITGB4 and EZR proteins. (B) Co-immunofluorescence staining in SW480 cells showing the co-localization of ITGB4 (green) and EZR (red) at the cell membrane. Nuclei were stained with DAPI (blue). (C) Protein-protein interaction network from the STRING database predicting an association between ITGB4 and EZR. (D and E) Verification of EZR overexpression efficiency in SW480 and HCT116 cells by RT-qPCR and western blot after transfection with pcDNA3.1-EZR. (F and G) RT-qPCR and western blot analysis showing decreased EZR mRNA and protein levels in SW480 cells after ITGB4 knockdown. (H and I) Western blot and RT-qPCR analysis confirming that EZR overexpression does not rescue the siRNA-mediated knockdown of ITGB4, indicating EZR acts downstream of ITGB4. Data are presented as the mean ± SD. *P<0.05, **P<0.01, ***P<0.001 and ****P<0.0001. ITGB4, integrin beta 4; EZR, Ezrin; RT-qPCR, reverse transcription-quantitative PCR; si-, small interfering; NC, negative control.

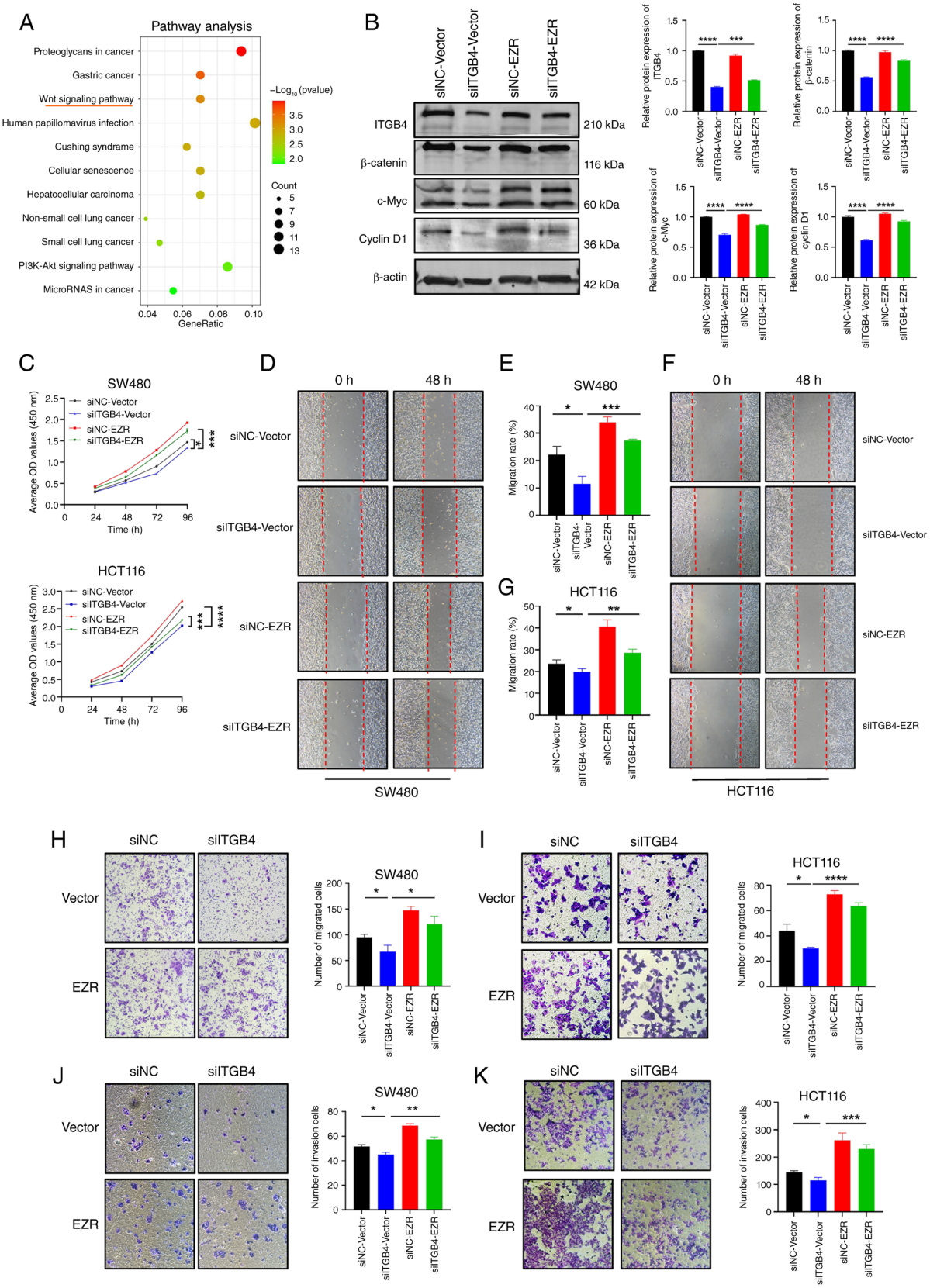

Figure 7. ITGB4 exerts its oncogenic function through the EZR-mediated activation of the Wnt/β-catenin signaling pathway. (A) Kyoto Encyclopedia of Genes and Genomes pathway enrichment analysis of differentially expressed genes following ITGB4 knockdown, highlighting the Wnt signaling pathway. (B) Western blot analysis and corresponding quantification showing that ITGB4 knockdown suppresses the expression of β-catenin, c-Myc and Cyclin D1, and this effect is rescued by EZR overexpression in HCT116 cells. (C) Cell Counting Kit-8 assays demonstrating that EZR overexpression rescues the proliferation defect caused by ITGB4 knockdown in SW480 and HCT116 cells. (D-G) Wound healing assays showing that EZR overexpression restores the migratory capacity inhibited by ITGB4 knockdown (magnification, x200). (H and I) Transwell migration assays confirming the rescue of cell migration by EZR overexpression (crystal violet staining; scale bar, 100 μm). (J and K) Transwell invasion assays showing that EZR overexpression rescues the invasive potential suppressed by ITGB4 knockdown (crystal violet staining; scale bar, 100 μm). Data are presented as the mean ± SD. *P<0.05, **P<0.01, ***P<0.001 and ****P<0.0001. ITGB4, integrin beta 4; EZR, Ezrin; si-, small interfering; NC, negative control.

overexpression of EZR significantly rescued these phenotypes. Taken together, these results demonstrate that ITGB4 promotes CRC progression by regulating EZR, which in turn leads to the activation of the Wnt/β-catenin signaling cascade.

Discussion

In the present study, a novel molecular mechanism underlying the pro-tumorigenic role of ITGB4 in CRC was elucidated. It was confirmed that ITGB4 is significantly overexpressed in CRC tissues and that its high expression is associated with poor patient prognosis. Through a series of *in vitro* and *in vivo* experiments, it was demonstrated that ITGB4 is critical for promoting CRC cell proliferation, migration, invasion and survival. Mechanistically, EZR was identified as a key downstream effector of ITGB4 for the first time. The current data reveal that ITGB4 interacts with and positively regulates EZR expression, which subsequently activates the Wnt/β-catenin signaling pathway, a well-established driver of CRC. These findings highlight the ITGB4/EZR/Wnt/β-catenin axis as a crucial signaling cascade in CRC progression and suggest its potential as a therapeutic target.

ITGB4, a transmembrane receptor, plays a pivotal role in cell-matrix adhesion and signal transduction (6). Its aberrant expression has been linked to the progression of various cancers (9-14). Consistent with these studies and the authors' previous findings (16), the present study solidifies the oncogenic function of ITGB4 in CRC. The functional experiments clearly demonstrated that silencing ITGB4 potently inhibits key malignant phenotypes, including proliferation and invasion, both in cultured cells and in a xenograft tumor model. These results strongly support ITGB4's role as a driver of CRC and reinforce its value as a potential therapeutic target.

A key innovation of the present study is the identification of EZR as a downstream target regulated by ITGB4. EZR is a member of the ERM protein family that links the plasma membrane to the actin cytoskeleton, thereby regulating cell adhesion, migration and signaling (20). EZR is known to be overexpressed in numerous malignancies, including CRC, where its expression correlates with advanced stage, metastasis and poor prognosis (21-25). While both ITGB4 and EZR have been independently implicated in cancer, a direct regulatory link between them in the context of CRC has not been previously described. The present study provides compelling evidence for this connection through Co-IP and Co-IF experiments demonstrating their physical interaction and co-localization. The co-localization of ITGB4 and EZR at the plasma membrane is biologically significant. As a transmembrane receptor, ITGB4 requires membrane-proximal effectors to transmit extracellular signals. EZR, serving as a cross-linker between the plasma membrane and the actin cytoskeleton, is ideally positioned to transduce ITGB4-mediated signals to the intracellular machinery. Furthermore, it was identified that ITGB4 expression level directly influences EZR mRNA and protein levels, suggesting that ITGB4 may regulate EZR through transcriptional or post-transcriptional mechanisms. While the precise mode of this regulation (for example, via downstream transcription factors or effects on mRNA stability) warrants further investigation, the present results firmly place EZR as a downstream mediator of ITGB4's oncogenic signaling.

The activation of the Wnt/β-catenin signaling pathway is a hallmark event in the majority of CRC, driving uncontrolled cell proliferation and survival (26,27). The pathway culminates in the nuclear translocation of β-catenin, which acts as a co-activator for TCF/LEF transcription factors to induce the expression of target genes such as c-Myc and Cyclin D1 (28). The present study connects the ITGB4/EZR axis to this critical pathway. It was demonstrated that ITGB4 knockdown deactivates the Wnt/β-catenin pathway and that this effect is mediated by EZR, as EZR overexpression could restore pathway activity. This finding is particularly significant as it provides a mechanistic explanation for how an upstream cell adhesion molecule such as ITGB4 can influence a core intracellular oncogenic signaling cascade. The ability of EZR to rescue the malignant phenotypes suppressed by ITGB4 knockdown further solidifies the functional importance of this newly identified axis. Furthermore, the current data serendipitously revealed that EZR overexpression could partially restore ITGB4 levels. Since β-catenin acts as a prominent transcription factor, it was hypothesized that ITGB4 could be a transcriptional target of the Wnt/β-catenin pathway. This potential positive feedback loop (ITGB4/EZR/Wnt/β-catenin/ITGB4) may continuously fuel CRC progression, which remains an intriguing hypothesis that warrants dedicated exploration and direct transcriptional validation in future studies.

Mechanistically, EZR may activate Wnt signaling through several potential pathways. A previous study in osteosarcoma indicated that EZR can physically interact with β-catenin and facilitate its nuclear translocation (29). Alternatively, EZR may disrupt the E-cadherin/β-catenin complex at the cell membrane, releasing a pool of β-catenin that acts as a signaling molecule rather than an adhesion component. Furthermore, EZR phosphorylation is a key regulatory event that modulates multiple downstream signaling cascades, including those that converge on β-catenin stability (30). The present findings in CRC are consistent with these models, suggesting that EZR acts as a critical signal transducer.

While other integrins, such as Beta 1, have been reported to modulate Wnt signaling via focal adhesion kinase, the ITGB4-mediated regulation appears distinct. Unlike Beta 1, ITGB4 primarily forms hemidesmosomes. The current data suggests that in cancer cells, ITGB4 signaling is re-wired away from stable adhesion towards pro-migratory signaling via EZR, a mechanism that may be unique to the structural properties of the Beta 4 subunit.

Nevertheless, the present study has certain limitations. First, while a regulatory relationship was demonstrated, the precise molecular details of how ITGB4 modulates EZR expression require further exploration. Future studies could investigate whether ITGB4 signaling affects transcription factors that bind to the EZR promoter or influences the stability of EZR mRNA. Second, the clinical correlation between ITGB4 and EZR expression should be validated in a larger cohort of CRC patient samples to strengthen its clinical relevance. Additionally, while *in vitro* assays strongly support a role for ITGB4 in migration and invasion, the subcutaneous xenograft model used in the present study primarily assesses tumor growth. Future studies utilizing

orthotopic implantation or tail vein injection models are necessary to fully validate the metastatic potential of the ITGB4/EZR axis *in vivo*. Despite these limitations, the present study provides a robust foundation for future research.

In conclusion, the present study identifies ITGB4 as a critical oncogene in CRC that promotes tumor progression by upregulating its downstream target EZR, leading to the activation of the Wnt/β-catenin signaling pathway. This newly defined ITGB4/EZR/Wnt/β-catenin axis offers novel insights into the molecular pathogenesis of CRC and presents ITGB4 as a promising biomarker for prognosis and a potential target for therapeutic intervention.

Acknowledgements

Not applicable.

Funding

The present study was supported by the Hebei Provincial Government-funded Provincial Medical Excellent Talent Project (grant nos. ZF2023025, ZF2024134, ZF2025045, ZF2025048, ZF2025051, LS202208 and LS202212), the Hebei Natural Science Foundation (grant nos. H2022206292 and H2024206140), the Key R&D Program of Hebei (grant nos. 223777103D and 223777113D), the Hebei County General Hospital Appropriate Health Technology Promotion Project (grant no. 20220018), the Prevention and treatment of geriatric diseases by Hebei Provincial Department of Finance (grant nos. LNB202202, LNB201809 and LNB201909), the Spark Scientific Research Project of the First Hospital of Hebei Medical University (grant nos. XH202312 and XH201805), the Hebei Medical Applicable Technology Tracking Project (grant no. G2019035) and other projects of Hebei (grant nos. 1387 and SGH201501).

Availability of data and materials

The data generated in the present study may be found in the Gene Expression Omnibus under accession number GSE326923 or at the following URL: https://www.ncbi.nlm.nih.gov/geo/query/acc.cgi?acc=GSE326923. The data generated in the present study may be requested from the corresponding author.

Authors' contributions

WY, JiaW and TL conceived and designed the study. JinW, YS and MX performed the experiments, analyzed the data, and wrote the manuscript. SH, KL and JJ provided technical support and study materials. XM and HL contributed to data collection and assembly. All authors read and approved the final version of the manuscript. JinW and YS confirm the authenticity of all the raw data.

Ethics approval and consent to participate

All animal procedures were approved by the Experimental Animal Care and Use Committee and the Ethics Committee of The First Hospital of Hebei Medical University (approval no. 20220395; Shijiazhuang, China). The study was carried out in compliance with the ARRIVE guidelines and all methods were performed in accordance with the relevant guidelines and regulations.

Patient consent for publication

Not applicable.

Competing interests

The authors declare that they have no competing interests.

References

1. Sung H, Ferlay J, Siegel RL, Laversanne M, Soerjomataram I, Jemal A and Bray F: Global cancer statistics 2020: GLOBOCAN estimates of incidence and mortality worldwide for 36 cancers in 185 countries. CA Cancer J Clin 71: 209-249, 2021.
2. Biller LH and Schrag D: Diagnosis and treatment of metastatic colorectal cancer: A review. JAMA 325: 669-685, 2021.
3. Winkler J, Abisoye-Ogunniyan A, Metcalf KJ and Werb Z: Concepts of extracellular matrix remodelling in tumour progression and metastasis. Nat Commun 11: 5120, 2020.
4. Janiszewska M, Primi MC and Izard T: Cell adhesion in cancer: Beyond the migration of single cells. J Biol Chem 295: 2495-2505, 2020.
5. Han S, Jiang X, Sun XF, Zhang H, Li C, Zhao Z and Yu W: Application value of CyTOF 2 mass cytometer technology at single-cell level in human gastric cancer cells. Exp Cell Res 384: 111568, 2019.
6. Borradori L and Sonnenberg A: Structure and function of hemidesmosomes: More than simple adhesion complexes. J Invest Dermatol 112: 411-418, 1999.
7. Zhang W, Zhang B, Vu T, Yuan G, Zhang B, Chen X, Manne U and Datta PK: Molecular characterization of pro-metastatic functions of β4-integrin in colorectal cancer. Oncotarget 8: 92333-92345, 2017.
8. Zhong F, Lu HP, Chen G, Dang YW, Li GS, Chen XY, Qin YY, Yao YX, Zhang XG, Liang Y, *et al*: The clinical significance and potential molecular mechanism of integrin subunit beta 4 in laryngeal squamous cell carcinoma. Pathol Res Pract 216: 152785, 2020.
9. Desgrosellier JS and Cheresh DA: Integrins in cancer: Biological implications and therapeutic opportunities. Nat Rev Cancer 10: 9-22, 2010.
10. Boelens MC, van den Berg A, Vogelzang I, Wesseling J, Postma DS, Timens W and Groen HJ: Differential expression and distribution of epithelial adhesion molecules in non-small cell lung cancer and normal bronchus. J Clin Pathol 60: 608-614, 2007.
11. Chung J, Bachelder RE, Lipscomb EA, Shaw LM and Mercurio AM: Integrin (alpha 6 beta 4) regulation of eIF-4E activity and VEGF translation: A survival mechanism for carcinoma cells. J Cell Biol 158: 165-174, 2002.
12. Damhofer H, Medema JP, Veenstra VL, Badea L, Popescu I, Roelink H and Bijlsma MF: Assessment of the stromal contribution to Sonic Hedgehog-dependent pancreatic adenocarcinoma. Mol Oncol 7: 1031-1042, 2013.
13. Gan L, Meng J, Xu M, Liu M, Qi Y, Tan C, Wang Y, Zhang P, Weng W, Sheng W, *et al*: Extracellular matrix protein 1 promotes cell metastasis and glucose metabolism by inducing integrin β4/FAK/SOX2/HIF-1α signaling pathway in gastric cancer. Oncogene 37: 744-755, 2018.
14. Ni H, Dydensborg AB, Herring FE, Basora N, Gagné D, Vachon PH and Beaulieu JF: Upregulation of a functional form of the beta4 integrin subunit in colorectal cancers correlates with c-Myc expression. Oncogene 24: 6820-6829, 2005.
15. Jiang X, Wang J, Wang M, Xuan M, Han S, Li C, Li M, Sun XF, Yu W and Zhao Z: ITGB4 as a novel serum diagnosis biomarker and potential therapeutic target for colorectal cancer. Cancer Med 10: 6823-6834, 2021.

16. Li M, Jiang X, Wang G, Zhai C, Liu Y, Li H, Zhang Y, Yu W and Zhao Z: ITGB4 is a novel prognostic factor in colon cancer. J Cancer 10: 5223-5233, 2019.
17. Kechagia JZ, Ivaska J and Roca-Cusachs P: Integrins as biomechanical sensors of the microenvironment. Nat Rev Mol Cell Biol 20: 457-473, 2019.
18. García-Ortiz A and Serrador JM: ERM proteins at the crossroad of leukocyte polarization, migration and intercellular adhesion. Int J Mol Sci 21: 1502, 2020.
19. Livak KJ and Schmittgen TD: Analysis of relative gene expression data using real-time quantitative PCR and the 2(-Delta Delta C(T)) Method. Methods 25: 402-408, 2001.
20. Bretscher A: Fimbrin is a cytoskeletal protein that crosslinks F-actin in vitro. Proc Natl Acad Sci USA 78: 6849-6853, 1981.
21. Lugini L, Lozupone F, Matarrese P, Funaro C, Luciani F, Malorni W, Rivoltini L, Castelli C, Tinari A, Piris A, *et al*: Potent phagocytic activity discriminates metastatic and primary human malignant melanomas: A key role of ezrin. Lab Invest 83: 1555-1567, 2003.
22. Kim C, Shin E, Hong S, Chon HJ, Kim HR, Ahn JR, Hong MH, Yang WI, Roh JK and Rha SY: Clinical value of ezrin expression in primary osteosarcoma. Cancer Res Treat 41: 138-144, 2009.
23. Krishnan K, Bruce B, Hewitt S, Thomas D, Khanna C and Helman LJ: Ezrin mediates growth and survival in Ewing's sarcoma through the AKT/mTOR, but not the MAPK, signaling pathway. Clin Exp Metastasis 23: 227-236, 2006.
24. Zhang Q, Ye Z, Zhang Y and Liao F: The expression and clinical significance of Ezrin and MMP-9 in colorectal cancer tissue. Altern Ther Health Med: Jun 28, 2024 (Epub ahead of print).
25. Liang F, Wang Y, Shi L and Zhang J: Association of Ezrin expression with the progression and prognosis of gastrointestinal cancer: A meta-analysis. Oncotarget 8: 93186-93195, 2017.
26. Tejeda-Muñoz N and Mei KC: Wnt signaling in cell adhesion, development, and colon cancer. IUBMB Life 76: 383-396, 2024.
27. Zhao H, Ming T, Tang S, Ren S, Yang H, Liu M, Tao Q and Xu H: Wnt signaling in colorectal cancer: Pathogenic role and therapeutic target. Mol Cancer 21: 144, 2022.
28. Jiang J, Li J, Yao W, Wang W, Shi B, Yuan F, Dong J and Zhang H: FOXC1 Negatively Regulates DKK1 expression to promote gastric cancer cell proliferation through activation of wnt signaling pathway. Front Cell Dev Biol 9: 662624, 2021.
29. Li X, Wang J, Long H, Lin W, Wang H, Chen Y, Yuan Q and Li X: circCDYL2, overexpressed in highly migratory colorectal cancer cells, promotes migration by binding to Ezrin. Front Oncol 11: 716073, 2021.
30. Song Y, Ma X, Zhang M, Wang M, Wang G, Ye Y and Xia W: Ezrin mediates invasion and metastasis in tumorigenesis: A review. Front Cell Dev Biol 8: 588801, 2020.